AGU PUBLICATIONS

Geophysical Research Letters

RESEARCH LETTER
10.1002/2014GL061489

Key Points:
- Cyclones encounter more lingering wakes with increasing cyclone frequency
- Cyclone-cyclone interactions reduce the mean cyclone intensification rates
- Cyclones may self-regulate their activity on intraseasonal time scale

Supporting Information:
- Readme
- Text S1
- Figure S1
- Figure S2

Correspondence to:
L. R. Leung,
Ruby.Leung@pnnl.gov

Citation:
Balaguru, K., S. Taraphdar, L. R. Leung, G. R. Foltz, and J. A. Knaff (2014), Cyclone-cyclone interactions through the ocean pathway, *Geophys. Res. Lett.*, *41*, 6855–6862, doi:10.1002/2014GL061489.

Received 12 AUG 2014
Accepted 18 SEP 2014
Accepted article online 23 SEP 2014
Published online 13 OCT 2014

Cyclone-cyclone interactions through the ocean pathway

Karthik Balaguru[1,2], Sourav Taraphdar[2], L. Ruby Leung[2], Gregory R. Foltz[3], and John A. Knaff[4]

[1]Coastal Sciences Division, Pacific Northwest National Laboratory, Seattle, Washington, USA, [2]Atmospheric Sciences and Global Change, Pacific Northwest National Laboratory, Richland, Washington, USA, [3]Physical Oceanography Division, Atlantic Oceanographic and Meteorological Laboratory, NOAA, Miami, Florida, USA, [4]NOAA Center for Satellite Applications and Research, Fort Collins, Colorado, USA

Abstract The intense sea surface temperature cooling caused by tropical cyclone-induced mixing lasts several weeks and may thus influence a later cyclone passing over it. Using a 28 year analysis spanning the North Atlantic, eastern Pacific, and Northwest Pacific, we systematically demonstrate that, on average, when tropical cyclones encounter lingering wakes, they experience sea surface temperatures that are ~0.25–0.5°C colder. Consequently, the intensification rates are ~0.4–0.7 $\frac{\mathrm{m\ s^{-1}}}{36\ \mathrm{h}}$ lower for cyclones when they interact with wakes, consistent with the maximum potential intensity theory. The probability for cyclones to encounter lingering wakes varies positively with cyclone frequency, is ~10% on average, and has been as high as 27%–37% in the past. These large interaction probabilities reduce the mean intensification rates for cyclones by 3%–6% on average and by ~12%–15% during the most active years. "Cyclone-cyclone interactions" may therefore represent a mechanism through which tropical cyclones self-regulate their activity to an extent on intraseasonal time scales.

1. Introduction

Tropical cyclones (hereafter "cyclones") are one of the most destructive and widespread natural hazards in the tropics and subtropics [*Emanuel*, 2003], with considerable socio-economic impact and the potential to actively modulate climate [*Sriver and Huber*, 2007; *Korty et al.*, 2008; *Mei et al.*, 2013]. Theory shows that the maximum wind speed that can be achieved by a cyclone depends critically on the air-sea temperature difference, making sea surface temperature (SST) one of the most important parameters to affect cyclone intensity [*Emanuel*, 1999]. Although the significance of SST has been further accentuated by studies showing that the integrated intensity of cyclones is strongly regulated by tropical SSTs at decadal time scales [*Emanuel*, 2005; *Sriver and Huber*, 2006], the contribution of SST to trends in cyclone activity remains uncertain, with studies yielding mixed results [*Knutson et al.*, 2010; *Vecchi and Knutson*, 2011; *Kossin et al.*, 2013].

When over the ocean, a cyclone induces intense vertical mixing that entrains colder, deeper water into the relatively warm mixed layer [*Price*, 1981; *Bender and Ginis*, 2000]. The pronounced SST cooling that results affects the evolution of the cyclone's intensity through modulation of air-sea enthalpy fluxes [*Shay et al.*, 2000; *Cione and Uhlhorn*, 2003; *Lin et al.*, 2008; *Lloyd and Vecchi*, 2011; *Balaguru et al.*, 2012]. These cold SST wakes relax back to climatological conditions at time scales of several weeks, opening up the possibility for later cyclones to interact with them [*Hart et al.*, 2007; *Price et al.*, 2008; *Dare and McBride*, 2011; *Vincent et al.*, 2012]. A very recent example of such an interaction occurred when cyclones Iselle and Julio approached the Hawaiian Islands in August 2014 (http://pmm.nasa.gov/mission-updates/trmm-news/trmm-sees-iselle-and-julio-menacing-hawaii).

The purpose of the present study is to systematically identify such interactions and quantify their impacts on cyclone intensity through the use of numerical model simulations of a representative case and historical observations. The layout of the paper is as follows. In section 2, a brief description of the numerical model, data, and methodology is given. Section 3 concerns the results obtained, and finally, the implications of our study are discussed in section 4.

2. Model, Data, and Methodology

To illustrate the impacts of lingering cold wakes on the intensity of later cyclones that pass over them, we select a numerical modeling case study. Next, to generalize the results, we analyze observed cyclone track data and SST data to estimate the intensification rates for cyclones that encounter and do not encounter lingering cold wakes, focusing on three ocean basins with frequent cyclone activities. These estimates are then compared against theoretical values of maximum potential intensity based on SST. More details are provided in the subsections below.

2.1. Model

Numerical modeling of Katia and Maria, two Atlantic cyclones during the 2011 cyclone season, was used to illustrate the mechanism of cyclone-cyclone interactions. Katia was a powerful Atlantic cyclone that caused considerable SST cooling in its wake, and Maria was a later cyclone that closely followed Katia's track and crossed over it. To evaluate the effects of Katia's cooling on Maria's intensity, numerical simulations were performed using the nonhydrostatic compressible WRF-ARW (Advanced Weather Research and Forecasting) model version 3.3.1 developed by National Center for Atmospheric Research [*Skamarock et al.*, 2005]. Two sets of simulations were conducted—control (WAKE) and experiment (NO-WAKE). In the WAKE set, the model is forced with observed SST, updated every 6 h. For the NO-WAKE set, we apply the same SST forcing as in WAKE but with a perturbation added to it that eliminates the fingerprint of Katia. The perturbation on 11 September, which is day 1 of the WAKE and NO-WAKE simulations, is given by the magnitude of the anomalous SST cooling caused by Katia on 11 September (supporting information Figure S1). The amplitude of the perturbation on each day of the simulation is progressively reduced from its value on the previous day according to the composite mean evolution of September SST anomalies (supporting information Figure S1). Each set includes 12 ensemble members, each member with a different combination of model physics parameterizations available in WRF to provide a more robust estimate of the effects of Katia's wake on Maria (supporting information).

2.2. Data

Cyclone track data for the period 1984–2011, obtained from http://eaps4.mit.edu/faculty/Emanuel [*Emanuel*, 2005], are used to identify cyclone track locations and maximum wind speed at 10 m, and to compute the cyclone translation speeds and intensification rates. The data here have been compiled from NOAA's National Hurricane Center [*Landsea and Franklin*, 2013] and from the U.S. Navy's Joint Typhoon Warning Center [*Chu et al.*, 2002]. Daily SST data from http://www.esrl.noaa.gov/psd/data [*Reynolds et al.*, 2007] are used to compute SST changes along the cyclone tracks. The domain of analysis is 15°N–25°N, 90°W–60°W in the Atlantic, 12°N–22°N, 120°W–100°W in the eastern Pacific, and 0°N–30°N, 130°E–180°E in the Northwest Pacific, respectively. The period of analysis is June–November for the Atlantic and Northwest Pacific basins and July–October for the eastern Pacific basin. These months correspond to the most active periods in each basin when interaction between cyclones is most likely. Additionally, in the Atlantic, we consider only those locations where the cyclone maximum wind speed exceeds 26 m s^{-1}. Subsampling cyclone track data using these regions, time periods, and minimum wind speed criteria ensures that the distribution of cyclone characteristics such as maximum wind speed and translation speed is statistically indistinguishable in the interacting and noninteracting sample sets, as confirmed by a Student's *t* test for difference of means. This allows for a fair comparison and makes our estimates of the effects of "cyclone-cyclone interactions" robust.

2.3. Methods

We identify cyclone-cyclone interactions from the historical data set of cyclone tracks for the period 1984–2011. For each cyclone track location, we check for later cyclone track locations that satisfy the "closeness in time," "closeness in space," and "minimum SST cooling" criteria. As the restoration time scale of a cyclone's cold SST wake is on the order of a few weeks [*Hart et al.*, 2007; *Price et al.*, 2008; *Dare and McBride*, 2011; *Vincent et al.*, 2012], to satisfy the closeness in time criterion, the maximum separation in time is taken as 2 weeks. The mean radius of 12 m s^{-1} surface wind for cyclones in the Atlantic, eastern Pacific, and Northwest Pacific is about 210 km, 125 km, and 250 km, respectively [*Chavas and Emanuel*, 2010]. Since little deep convection occurs beyond this distance from the center [*Chavas and Emanuel*, 2010], we assume this distance as the mean cyclone radius and twice this distance as the mean cyclone size in the corresponding basin. If the distance between the two cyclone track locations is less than the corresponding mean cyclone size for that basin, then the closeness in space criterion is satisfied. Finally, if the SST cooling induced by the

first cyclone is at least 0.5°C in magnitude, then the minimum SST cooling criterion is satisfied. This ensures that a significant amount of SST cooling induced by a prior cyclone persists beyond 2 weeks, as shown in section 3.2. If all three criteria are met, then a cyclone-cyclone interaction is said to occur.

Daily SST anomalies are computed by subtracting climatological daily SST values, generated using 28 years of SST data, from the corresponding daily SST values. The SST change under a cyclone is then given as the difference between the SST anomaly 2 days after the arrival of the storm and the 10 day mean SST anomaly prior to a day before the arrival of the storm. The values of SST change are averaged over a box centered on the storm. The size of the box in each basin is based on the mean cyclone size for the corresponding basin [*Chavas and Emanuel*, 2010; *Knaff and Zehr*, 2007; *Knaff et al.*, 2014]. This procedure accounts for any possible asymmetry in cyclones. The cyclone intensification rate is calculated as the linear regression coefficient of the maximum wind speed over six successive 6-hourly snapshots [*Lloyd and Vecchi*, 2011]. Track locations for cyclones making landfall within these 36 h are excluded from our analysis to eliminate possible contamination of our results from landfall effects. The histograms and probability density function (PDFs) have been estimated using the Monte Carlo technique of repeated random sampling [*Balaguru et al.*, 2012].

Having estimated the PDFs of cyclone intensification rate and probability of cyclone-cyclone interactions, the percentage reduction in the overall mean intensification rate due to cyclone-cyclone interactions is calculated as $\frac{p*(I_{nw}-I_w)}{I_{nw}}$, where p is the probability of interaction, I_{nw} is the mean intensification rate when wakes are not encountered, and I_w is the mean intensification rate when wakes are encountered. Additionally, the reduction in cyclone intensification rate can be estimated theoretically for comparison. Following *Cione and Uhlhorn* [2003], the potential intensity (PI) of a cyclone is defined as the difference between the SST-based maximum potential intensity (MPI) and the initial intensity of the cyclone before intensification. In the Atlantic and Northwest Pacific, the MPI is an exponential function of SST and is expressed as $\mathrm{MPI} = A + B.e^{C(\mathrm{SST}-T_0)}$. Here the constants A, B, C, and T_0 are obtained for the Atlantic and Northwest Pacific basins from *DeMaria and Kaplan* [1994] and *Zeng et al.* [2007], respectively. On the other hand, in the eastern Pacific, MPI varies linearly with SST and is given as $\mathrm{MPI} = C_0 + C_1(\mathrm{SST} - T_0)$. The constants C_0 and C_1 in this relationship are obtained from *Whitney and Hobgood* [1997]. We calculate the mean values of MPI across all cyclones, separated into those that encounter and those that do not encounter wakes.

3. Results

3.1. Case Study

We begin with the case study of Katia and Maria, two Atlantic cyclones that occurred between 29 August and 16 September 2011. The SST cooling induced by Katia is shown in Figure 1a with the tracks of Katia and Maria overlaid. Katia was a major cyclone that caused considerable SST cooling along its track in the northwestern tropical Atlantic. Maximum cooling of 3°C occurred near 65°W and 25°N, where Katia reached its peak intensity of category 4 on the Saffir-Simpson scale. Maria passed very close to the track of Katia between 11 and 14 September, separated by a maximum distance of 500 km, and crossed directly over Katia's track on 15 September. Thus, it is likely that during this period, Maria, which remained at "tropical storm" strength throughout, felt the lingering cold SST wake of Katia. The time evolution of SST cooling induced by Katia (Figure 1b) shows that maximum cooling occurred between 9 and 10 September and between 65°W and 70°W. Later, considerable SST cooling induced by Katia persisted until the arrival of Maria, despite a decrease in the magnitude of the cooling.

Having established that Maria felt the cold SST wake of Katia, we next evaluate the impact of the wake on Maria's intensity through an ensemble of numerical sensitivity experiments with an atmospheric model. For the control case (WAKE), in which the model is forced with observed SST, the salient features of Maria are reasonably reproduced (supporting information). In the experiment case (NO-WAKE), the model is forced with SST that has the influence of Katia removed. Consequently, Maria's maximum intensity in NO-WAKE is higher, as depicted in Figure 1c. Maria's intensity gradually increases in NO-WAKE beginning on 12 September, as the storm makes its way closer to the region where Katia's cooling was strong. Maria achieves a category 2 intensity by 18:00 UTC of 14 September in NO-WAKE, considerably stronger than the category 1 intensity reached in WAKE. The enthalpy flux at the air-sea interface under Maria is 55 W m^{-2} higher between 13 and 15 September for NO-WAKE compared to WAKE, due to the absence of Katia's cold wake. As a result, in NO-WAKE the maximum wind speed is 10 m s^{-1} higher and the minimum sea level pressure (SLP) is 14 hPa lower on average compared to WAKE. The differences between the experiments are

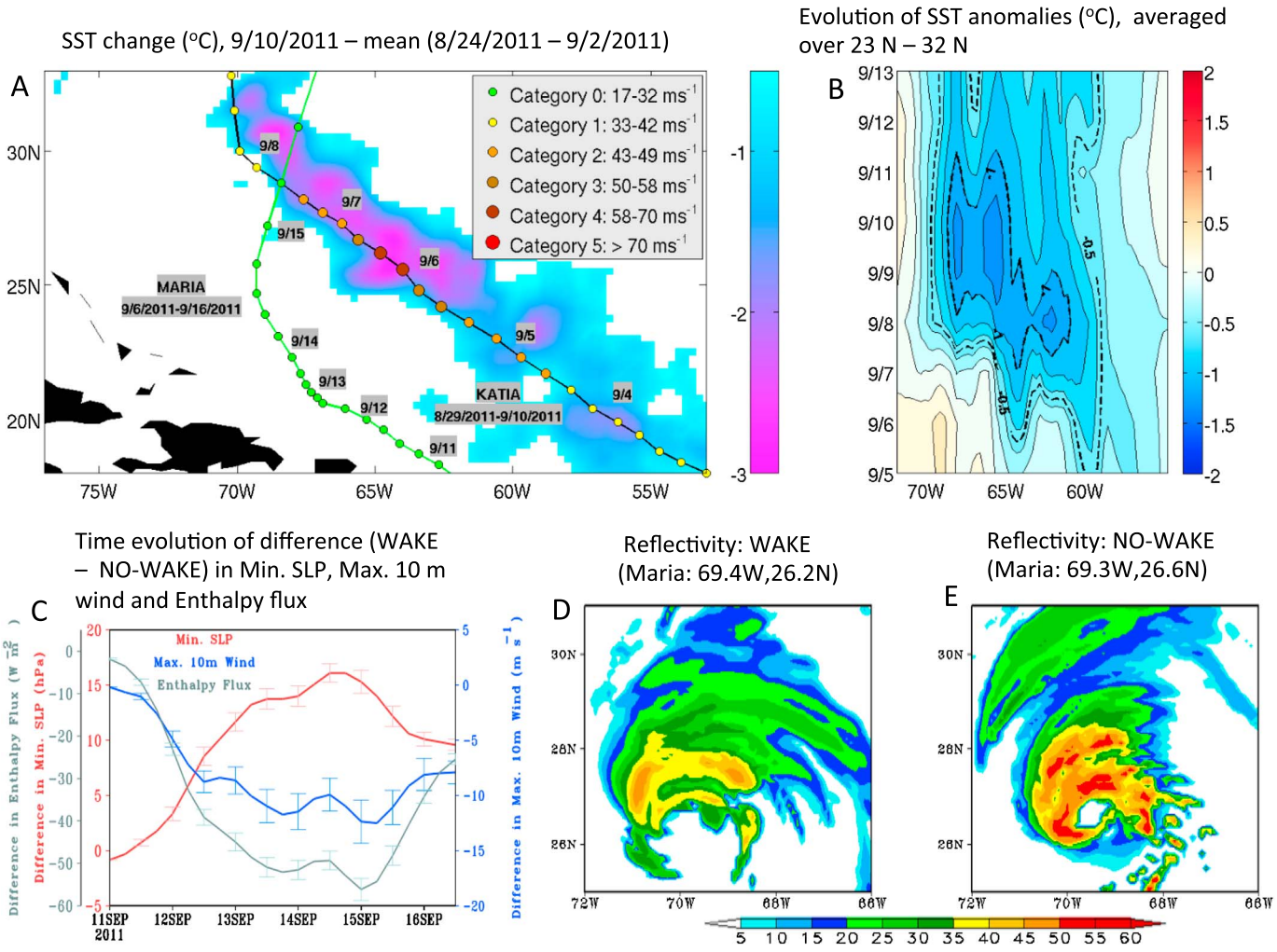

Figure 1. Interaction of cyclones Katia and Maria. (a) The SST cooling induced by Katia is shown in the background with the tracks of cyclones Katia and Maria overlaid. (b) The time evolution of SST cooling induced by Katia, averaged between 23°N and 32°N, is shown in this Hovmöller plot. SST evolution is shown only until 13 September, beyond which it is contaminated by Maria's wake. (c) Time evolution of the ensemble mean difference between WAKE and NO-WAKE for enthalpy flux, maximum 10 m wind speed and minimum sea level pressure (SLP) with error bars indicated. Snapshots of reflectivity at 12:00 UTC of 14 September from (d) WAKE and (e) NO-WAKE with the storm locations indicated. Note that the reflectivity in Figures 1d and 1e corresponds to the time when Maria began to cross Katia's wake in the model and also when the difference between Maria's intensity in the WAKE and NO-WAKE experiments was a maximum (Figure 1c). The slight discrepancy between the modeled and observed storm locations arises because the simulated translation speed of Maria is slightly faster than the observed speed.

further delineated in Figures 1d and 1e, which show snapshots of reflectivity, a proxy for the strength of atmospheric convection, at 12:00 UTC on 14 September. The convection of Maria in WAKE was disorganized, but it was well organized in NO-WAKE with a clearly defined eye and a concentric eyewall structure. Thus, the SST cooling induced by Katia limited the maximum intensity and intensification rate of Maria.

3.2. Observational Analysis

The case study of Katia and Maria leads to the following questions: Is this an isolated event or does it occur more often for cyclones in general? If so, how significant and frequent are these interactions and what are the broader implications? To address these questions, we perform a Lagrangian analysis of tropical storms and cyclones for the 28 year period 1984–2011 in the Atlantic and the eastern and Northwest Pacific basins, the three most active cyclone basins [*Gray*, 1968]. We define a cyclone-cyclone interaction as a situation in which a cyclone approaches another cyclone sufficiently close in time and space, to feel the cold SST wake induced by the first storm. We then compute preexisting SST, the SST change induced by each cyclone and the cyclones' intensification rates, contrasting the situations in which cyclones encounter wakes with cases in which they do not.

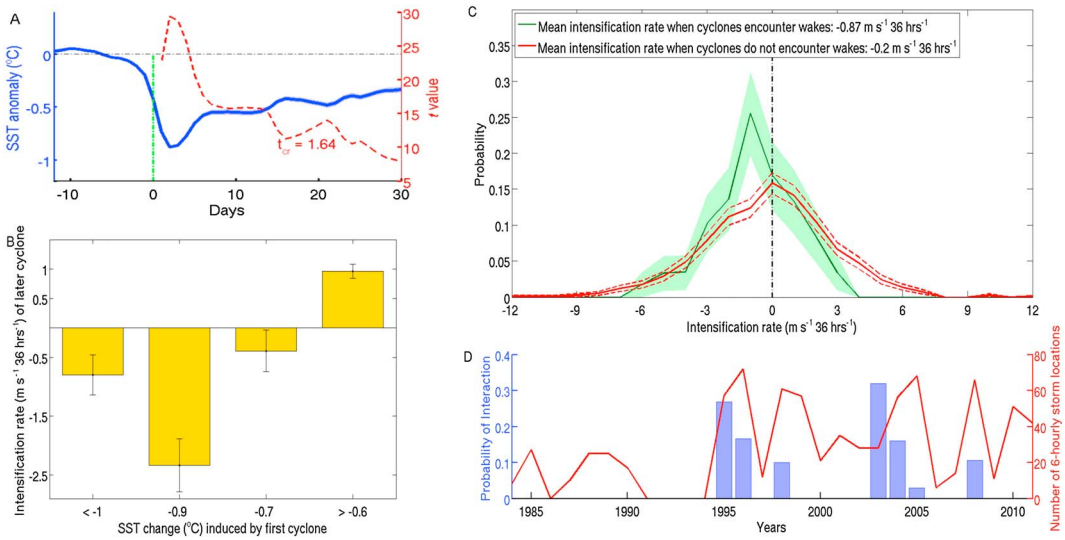

Figure 2. Analysis of Atlantic cyclone track data (1984–2011). (a) Composite mean evolution of cyclone-induced SST anomalies colder than −0.5°C. (b) Mean intensification rate of a later storm as a function of the SST change induced by the first storm. (c) PDF of intensification rates for cyclones when they encounter cold wakes and when they do not. The lighter shading indicates the error bounds. (d) The probability for cyclone-cyclone interactions and the number of 6-hourly cyclone track locations. The region of analysis in the Atlantic is bounded by 90°W–60°W and 15°N–25°N.

The mean SST felt by cyclones when they encounter wakes is lowered by 0.53°C in the Atlantic, 0.38°C in the eastern Pacific, and 0.25°C in the Northwest Pacific compared to the SST when they do not encounter wakes. The larger magnitude of cold wakes in the Atlantic reflects a higher threshold for wind speed used for subsampling data in that basin. Thus, when cyclones encounter wakes, there is a reduction in the amount of energy in the upper ocean that can be transferred to the storm and aid its intensification. The consequent effect is illustrated in Figures 2, 3, and 4 for the Atlantic, the eastern, and Northwest Pacific basins, respectively. Composite mean profiles of the evolution of SST cooling reveal that the surface ocean cooling induced by cyclones is significant well beyond 30 days on average (Figures 2a, 3a, and 4a), providing a window of time for interactions to occur.

The histogram of mean intensification rates when cyclones encounter wakes is plotted as a function of the SST change induced by earlier cyclones (Figures 2b, 3b, and 4b). In general, the larger the magnitude

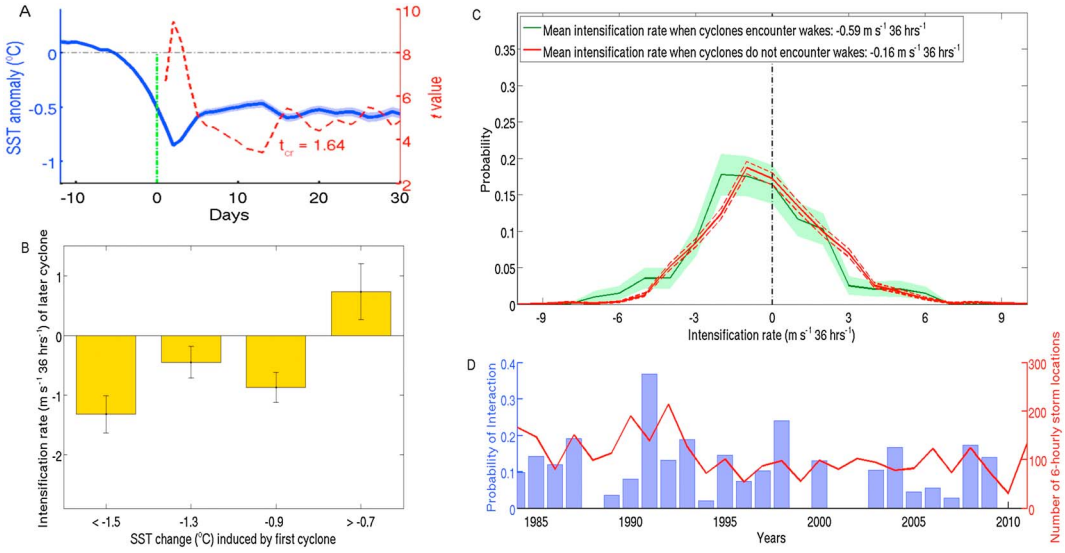

Figure 3. Analysis of eastern Pacific cyclone track data (1984–2011). As in Figure 2 but for the eastern Pacific. The region of analysis is bounded by 120°W–100°W and 12°N–22°N.

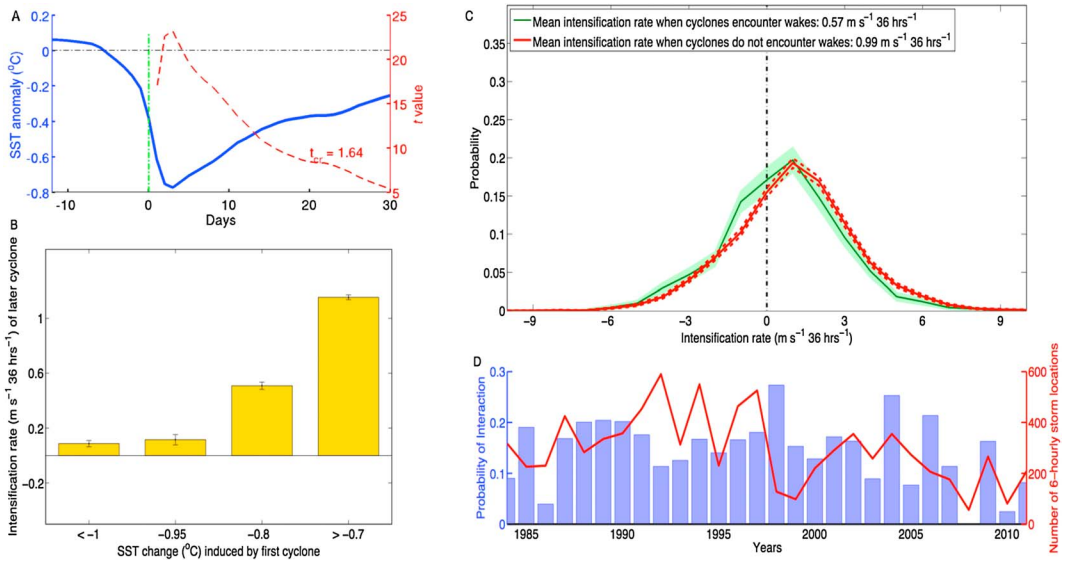

Figure 4. Analysis of Northwest Pacific cyclone track data (1984–2011). As in Figure 2 but for Northwest Pacific. The region of analysis is bounded by 130°E–180°E and 0°N–30°N.

of SST cooling produced by the prior cyclones, the stronger the decay of later cyclones when they encounter the wakes. Probability distribution functions (PDFs) of intensification rates are derived from data for cyclones when they encounter cold wakes and when they do not (Figures 2c, 3c, and 4c). The PDFs for cyclones when they encounter wakes are skewed toward lower intensification rates compared to the PDFs for cyclones when they do not. For the Atlantic, the mean intensification rate for cyclones when they encounter wakes is $-0.87\ \frac{\text{m s}^{-1}}{36\,\text{h}}$, whereas for cyclones when they do not encounter wakes the rate is considerably higher at $-0.2\ \frac{\text{m s}^{-1}}{36\,\text{h}}$. Similarly, for the eastern and Northwest Pacific, the mean intensification rates for cyclones when they encounter wakes are $-0.59\ \frac{\text{m s}^{-1}}{36\,\text{h}}$ and $0.57\ \frac{\text{m s}^{-1}}{36\,\text{h}}$, substantially lower than the mean intensification rates when they do not encounter wakes, which are $-0.16\ \frac{\text{m s}^{-1}}{36\,\text{h}}$ and $0.99\ \frac{\text{m s}^{-1}}{36\,\text{h}}$, respectively. These results emphasize the weakening effect of wakes on cyclones when they encounter them. The differences in SST and cyclone intensification rates with and without wakes are statistically significant at the 95% confidence level.

To further understand these changes in intensification rates, we consider the impact of cold wakes on the PI, a measure of a cyclone's intensification tendency. Since our primary aim is to isolate the influence of cold SST wakes, we use the form of MPI that is a function of SST alone. According to this formulation, the MPI denotes the upper bound to the intensity that can be achieved by a cyclone for a given SST. Hence, under identical initial intensity conditions, the change in PI for a storm due to a difference in SST is equivalent to the change in MPI. Using this relationship, the difference in PI for cyclones when they encounter and do not encounter wakes is estimated from the corresponding mean SST felt by cyclones. For instance, the reduction in PI caused by wakes in the Atlantic is computed as 4.2 m s^{-1}. Assuming that this reduction occurs over 36 h or six 6-hourly time steps, it translates into a decay rate of $0.7\ \frac{\text{m s}^{-1}}{36\,\text{h}}$, which compares very well with the difference in mean intensification rates for cyclones when they interact and do not interact with wakes, obtained from actual calculations (Table 1). Similar consistency is obtained for both the eastern Pacific and Northwest Pacific cyclone basins. These results firmly reinforce our hypothesis that interaction with lingering cold wakes from prior cyclones considerably reduces the intensification rates of cyclones.

The probability for cyclones to encounter lingering cold wakes varies positively with cyclone frequency in all three basins. Consistent with cyclone activity, in the Atlantic the chance to encounter wakes exhibits considerable year-to-year variability with a maximum of 28% and a mean of 7.5% (Figure 2d). In the eastern Pacific basin, which is the second most significant basin in terms of active storm area [*Gray*, 1968], the probability for cyclones to interact with wakes is 11% on average and has been as high as 37% (Figure 3d). The Northwest Pacific is by far the most active cyclone basin and accounts for nearly one third of the global cyclone activity [*Gray*, 1968]. The probability for cyclones to encounter wakes in this basin is nearly 15%

Table 1. Summary of Impact of "Cyclone-Cyclone" Interactions in Each Ocean Basin

	Atlantic	Eastern Pacific	Northwest Pacific
Mean SST felt—wake	28.11°C	27.07°C	28.40°C
Mean SST felt—no wake	28.64°C	27.45°C	28.64°C
Mean reduction in SST due to wakes	0.53°C	0.38°C	0.25°C
Mean reduction in MPI due to wakes	4.22 m s^{-1}	2.08 m s^{-1}	3.27 m s^{-1}
Mean intensification rate—wake	$-0.87\ \frac{m\ s^{-1}}{36\ h}$	$-0.6\ \frac{m\ s^{-1}}{36\ h}$	$0.57\ \frac{m\ s^{-1}}{36\ h}$
Mean intensification rate—no wake	$-0.21\ \frac{m\ s^{-1}}{36\ h}$	$-0.16\ \frac{m\ s^{-1}}{36\ h}$	$0.99\ \frac{m\ s^{-1}}{36\ h}$
Mean reduction in intensification rate due to wakes	$0.67\ \frac{m\ s^{-1}}{36\ h}$	$0.44\ \frac{m\ s^{-1}}{36\ h}$	$0.42\ \frac{m\ s^{-1}}{36\ h}$
Mean interaction probability	7.5%	11%	15.4%
Maximum interaction probability	28%	37%	27%

on average and has been as high as 27% in the past (Figure 4d). These interaction probabilities are large enough to modulate the mean intensification rates for cyclones. On average, cyclone-cyclone interactions reduce the intensification rates for cyclones by 3.2% in the Atlantic, 4.6% in the eastern Pacific, and 6.5% in the Northwest Pacific. Furthermore, during the most active years, the mean intensification rates are reduced by as much as ~12% in the Atlantic and Northwest Pacific, and by ~15% in the eastern Pacific. A summary of the statistics for each cyclone basin is provided in Table 1. (Note that the above values for the mean and maximum interaction probabilities are based on subsampled data in the three basins. When basin-wide cyclone-cyclone interactions are considered, the interaction probabilities are considerably higher (supporting information)).

4. Discussion

The analyses and ideas presented here represent a shift in our understanding of cyclone-cyclone interactions, from infrequent events that may affect an individual cyclone's intensity to a mechanism that significantly modulates cyclone activity at intraseasonal time scales. Few studies in the past discussed the possibility that cyclones may moderate the environment for subsequent cyclones [*Brand*, 1971; *Bender and Ginis*, 2000; *Hart et al.*, 2007; *Wada and Usui*, 2007; *Baranowski et al.*, 2014]. The below normal September Atlantic cyclone activity in 1995 has been partly attributed to the intense activity during the previous month of August [*Landsea et al.*, 1998]. Our analysis (Figure 2d) shows that the Atlantic experienced many cyclone-cyclone interactions during 1995, providing support to the argument. Some other studies also speculated on the possibility that interactions between cyclones through the ocean pathway may play a role in the intraseasonal variability of cyclone activity [*Knaff et al.*, 2013]. However, this study is the first to present comprehensive and quantitative evidence.

Finally, there are a few caveats in our present work. Variations in cyclone size [*Knaff et al.*, 2014] and lasting changes in atmospheric stability [*Hart et al.*, 2007] were not evaluated in this study. Next, we use the SST cooling induced by a cyclone as a measure of its wake and assume that the recovery of the SST cooling signifies that of the wake. However, in reality the upper ocean cooling extends several tens of meters below the surface and persists beyond the SST recovery time scale [*Mrvaljevic et al.*, 2013]. Hence, by considering only the SSTs, we may have underestimated the full impact of cyclone-cyclone interactions. Lastly, though we demonstrate the ability of cyclones to check their own activity at subseasonal time scales, it is not clear how this process influences the long-term variability of cyclones as a system. Mounting evidence suggests that cyclone-induced vertical mixing may induce a warming in the ocean subsurface that persists for several months [*Sriver and Huber*, 2007; *Mei et al.*, 2013]. These warm anomalies below the thermocline may reduce the entrainment cooling of the mixed layer for a later cyclone, tending to aid its intensification. Thus, the "ocean heat pump" induced by cyclones has the potential to overwhelm the impact of cold SST wakes at interannual to decadal time scales. Detailed modeling studies are therefore needed to understand the relative significance of these two mechanisms and the implications of their combined influence for future cyclone activity.

Acknowledgments
This research is based on work supported by the U.S. Department of Energy (DOE) Office of Science Biological and Environmental Research as part of the Regional and Global Climate Modeling program and the Integrated Assessment Research program. The Pacific Northwest National Laboratory is operated for DOE by Battelle Memorial Institute under contract DE-AC05-76RL01830. G.F. was funded by base funds to NOAA/AOML's Physical Oceanography Division. The views, opinions, and findings contained in this report are those of the authors and should not be construed as an official National Oceanic and Atmospheric Administration or U.S. Government position, policy, or decision.

Noah Diffenbaugh thanks Christopher Landsea and Matthew Huber for their assistance in evaluating this paper.

References

Balaguru, K., P. Chang, R. Saravanan, L. R. Leung, Z. Xu, M. Li, and J.-S. Hsieh (2012), Ocean barrier layers effect on tropical cyclone intensification, *PNAS*, *109*(36), 14,343–14,347.

Baranowski, D., P. J. Flatau, S. Chen, and P. Black (2014), Upper ocean response to the passage of two sequential typhoons, *Ocean Sci.*, *10*(3), 559–570.

Bender, M. A., and I. Ginis (2000), Real-case simulations of hurricane-ocean interaction using a high-resolution coupled model: Effects on hurricane intensity, *Mon. Weather Rev.*, *128*(4), 917–946.

Brand, S. (1971), The effects on a tropical cyclone of cooler surface waters due to upwelling and mixing produced by a prior tropical cyclone, *J. Appl. Meteorol.*, *10*(5), 865–874.

Chavas, D. R., and K. A. Emanuel (2010), A quikscat climatology of tropical cyclone size, *Geophys. Res. Lett.*, *37*(18), L18816, doi:10.1029/2010GL044558.

Chu, J.-H., C. R. Sampson, A. S. Levine, and E. Fukada (2002), The joint typhoon warning center tropical cyclone best-tracks, 1945–2000, *Tech. Rep. NRL/MR/7540-02-16*, Nav. Res. Lab., Monterey, Calif.

Cione, J. J., and E. W. Uhlhorn (2003), Sea surface temperature variability in hurricanes: Implications with respect to intensity change, *Mon. Weather Rev.*, *131*(8), 1783–1796.

Dare, R. A., and J. L. McBride (2011), Sea surface temperature response to tropical cyclones, *Mon. Weather Rev.*, *139*(12), 3798–3808.

DeMaria, M., and J. Kaplan (1994), Sea surface temperature and the maximum intensity of atlantic tropical cyclones, *J. Clim.*, *7*(9), 1324–1334.

Emanuel, K. (2003), Tropical cyclones, *Annu. Rev. Earth Planet. Sci.*, *31*(1), 75–104.

Emanuel, K. (2005), Increasing destructiveness of tropical cyclones over the past 30 years, *Nature*, *436*(7051), 686–688.

Emanuel, K. A. (1999), Thermodynamic control of hurricane intensity, *Nature*, *401*(6754), 665–669.

Gray, W. M. (1968), Global view of the origin of tropical disturbances and storms, *Mon. Weather Rev.*, *96*(10), 669–700.

Hart, R. E., R. N. Maue, and M. C. Watson (2007), Estimating local memory of tropical cyclones through MPI anomaly evolution, *Mon. Weather Rev.*, *135*(12), 3990–4005.

Knaff, J. A., and R. M. Zehr (2007), Reexamination of tropical cyclone wind-pressure relationships, *Weather Forecasting*, *22*(1), 71–88.

Knaff, J. A., M. DeMaria, C. R. Sampson, J. E. Peak, J. Cummings, and W. H. Schubert (2013), Upper oceanic energy response to tropical cyclone passage, *J. Clim.*, *26*(8), 2631–2650.

Knaff, J. A., S. P. Longmore, and D. A. Molenar (2014), An objective satellite-based tropical cyclone size climatology, *J. Clim.*, *27*(1), 455–476.

Knutson, T. R., J. L. McBride, J. Chan, K. Emanuel, G. Holland, C. Landsea, I. Held, J. P. Kossin, A. Srivastava, and M. Sugi (2010), Tropical cyclones and climate change, *Nat. Geosci.*, *3*(3), 157–163.

Korty, R. L., K. A. Emanuel, and J. R. Scott (2008), Tropical cyclone-induced upper-ocean mixing and climate: Application to equable climates, *J. Clim.*, *21*(4), 638–654.

Kossin, J. P., T. L. Olander, and K. R. Knapp (2013), Trend analysis with a new global record of tropical cyclone intensity, *J. Clim.*, *26*(24), 9960–9976.

Landsea, C. W., and J. L. Franklin (2013), Atlantic hurricane database uncertainty and presentation of a new database format, *Mon. Weather Rev.*, *141*(10), 3576–3592.

Landsea, C. W., G. D. Bell, W. M. Gray, and S. B. Goldenberg (1998), The extremely active 1995 atlantic hurricane season: Environmental conditions and verification of seasonal forecasts, *Mon. Weather Rev.*, *126*(5), 1174–1193.

Lin, I., C.-C. Wu, I.-F. Pun, and D.-S. Ko (2008), Upper-ocean thermal structure and the western North Pacific category 5 typhoons. Part I: Ocean features and the category 5 typhoons' intensification, *Mon. Weather Rev.*, *136*(9), 3288–3306.

Lloyd, I. D., and G. A. Vecchi (2011), Observational evidence for oceanic controls on hurricane intensity, *J. Clim.*, *24*(4), 1138–1153.

Mei, W., F. Primeau, J. C. McWilliams, and C. Pasquero (2013), Sea surface height evidence for long-term warming effects of tropical cyclones on the ocean, *PNAS*, *110*(38), 15,207–15,210.

Mrvaljevic, R. K., et al. (2013), Observations of the cold wake of typhoon Fanapi (2010), *Geophys. Res. Lett.*, *40*(2), 316–321, doi:10.1029/2012GL054282.

Price, J. F. (1981), Upper ocean response to a hurricane, *J. Phys. Oceanogr.*, *11*(2), 153–175.

Price, J. F., J. Morzel, and P. P. Niiler (2008), Warming of SST in the cool wake of a moving hurricane, *J. Geophys. Res.*, *113*(C7), C07010, doi:10.1029/2007JC004393.

Reynolds, R. W., T. M. Smith, C. Liu, D. B. Chelton, K. S. Casey, and M. G. Schlax (2007), Daily high-resolution-blended analyses for sea surface temperature, *J. Clim.*, *20*(22), 5473–5496.

Shay, L. K., G. J. Goni, and P. G. Black (2000), Effects of a warm oceanic feature on hurricane Opal, *Mon. Weather Rev.*, *128*(5), 1366–1383.

Skamarock, W. C., J. B. Klemp, J. Dudhia, D. O. Gill, D. M. Barker, W. Wang, and J. G. Powers (2005), A description of the advanced research WRF version 2, *Tech. Rep. DTIC Document*, National Center for Atmospheric Research, Boulder, Colo.

Sriver, R., and M. Huber (2006), Low frequency variability in globally integrated tropical cyclone power dissipation, *Geophys. Res. Lett.*, *33*(11), L11705, doi:10.1029/2006GL026167.

Sriver, R. L., and M. Huber (2007), Observational evidence for an ocean heat pump induced by tropical cyclones, *Nature*, *447*(7144), 577–580.

Vecchi, G. A., and T. R. Knutson (2011), Estimating annual numbers of atlantic hurricanes missing from the HURDAT database (1878-1965) using ship track density, *J. Clim.*, *24*(6), 1736–1746.

Vincent, E. M., M. Lengaigne, J. Vialard, G. Madec, N. C. Jourdain, and S. Masson (2012), Assessing the oceanic control on the amplitude of sea surface cooling induced by tropical cyclones, *J. Geophys. Res.*, *117*(C5), C05023, doi:10.1029/2011JC007705.

Wada, A., and N. Usui (2007), Importance of tropical cyclone heat potential for tropical cyclone intensity and intensification in the western North Pacific, *J. Oceanogr.*, *63*(3), 427–447.

Whitney, L. D., and J. S. Hobgood (1997), The relationship between sea surface temperatures and maximum intensities of tropical cyclones in the eastern North Pacific Ocean, *J. Clim.*, *10*, 2921–2930.

Zeng, Z., Y. Wang, and C.-C. Wu (2007), Environmental dynamical control of tropical cyclone intensity—An observational study, *Mon. Weather Rev.*, *135*(1), 38–59.